NJC

Accepted Manuscript

This is an *Accepted Manuscript*, which has been through the Royal Society of Chemistry peer review process and has been accepted for publication.

Accepted Manuscripts are published online shortly after acceptance, before technical editing, formatting and proof reading. Using this free service, authors can make their results available to the community, in citable form, before we publish the edited article. We will replace this *Accepted Manuscript* with the edited and formatted *Advance Article* as soon as it is available.

You can find more information about *Accepted Manuscripts* in the Information for Authors.

Please note that technical editing may introduce minor changes to the text and/or graphics, which may alter content. The journal's standard Terms & Conditions and the Ethical guidelines still apply. In no event shall the Royal Society of Chemistry be held responsible for any errors or omissions in this *Accepted Manuscript* or any consequences arising from the use of any information it contains.

ROYAL SOCIETY OF CHEMISTRY

www.rsc.org/njc

Electrical conductivity and Acetaldehyde vapours sensing studies on synthetic Polypyrrole-Titanium(IV)sulphosalicylophosphate nanocomposite cation exchange material.

Asif Ali Khan*, Rizwan Hussain, Shakeeba Shaheen

Analytical and Polymer Research Laboratory, Department of Applied Chemistry, Faculty of Engineering and Technology, Aligarh Muslim University, Aligarh-202002 (UP) INDIA

Abstract: In this study, a novel electrically conductive Polypyrrole-titanium(IV)sulphosalicylophosphate (PPy-TSCP) cation exchange nanocomposite has been synthesized by *in-situ* chemical oxidative polymerization of pyrrole in the presence of Titanium(IV)sulphosalicylophosphate (TSCP). PPy-TSCP cation exchange nanocomposite was characterized by various instrumentation techniques like FTIR, FE-SEM, XRD, TGA, DTA, DTG and EDX. The composite exhibited good ion-exchange capacity (IEC) (2.10 $meqg^{-1}$) as well as electrical conductivity (0.756 S/cm) and isothermal stability in terms of DC electrical conductivity retention under ambient condition up to 100 ˚C. PPy-TSCP cation exchange nanocomposite based sensor was fabricated for the detection of acetaldehyde vapors and it was found that the resistivity of the nanocomposites increases on exposure to high concentration of acetaldehyde vapors at room temperature (25 ˚C). The rate of reaction for acetaldehyde vapor sensing on PPy-TSCP was observed as first order.

Keywords: Polymer; Nanocomposite cation exchanger; Electrical conductivity; Vapour sensing

*Corresponding author's email: asifalikhan2008@gmail.com (A.A.Khan);

Tel.:+91-571-2720323

1. Introduction

Over the last decade the development of conducting nanocomposites have received great attention because of their interesting possibilities of structural modification and promising potential applications in chemistry, biology, medicine and material science **[1]**. Conducting nanocomposites with unique electrical, catalytic and optical properties are formed by combining a wide range of organic and nanoscale inorganic materials. Conducting polymers have inherent property to combine with different inorganic materials, because of their good electrical conductivity **[2]** they have wide applications in Sensors **[3-5]**, EMI shielding **[6],** light emitting diode **[7],** opto-electronics and energy storage devices **[8]** etc.

Electrical and Electrochemical properties of conducting polymers can be dramatically improved by forming composites of the conducting polymers and other materials such as carbon materials **[9]** metal oxides **[10-12]** and ion exchangers **[13]**. The synergistic associations of the integrated organic and inorganic materials have the merits of each component with the enhanced properties in composite materials **[14].**

Gas sensing applications of composite material have attracted great attention of researchers over the last few years **[15]**. The composite of metal oxides mixed with insulating polymer **[16]** and conducting polymer with carbon black **[17]** are of great interest these days, because they provide improve sensing responses to analyte gases as compared to their original components. Among various volatile organic compounds acetaldehyde is one of the classes of highly reactive organic compound, at one atmospheric pressure its boiling point is 20.2 $^{\circ}$C. Since it is extremely volatile liquid to produce vapours at room temperature, which are extremely irritating with characteristic pungent odor and may be some time harmful to human even at low concentration. Thus detection

and determination of aldehyde vapours in the atmosphere are of the immediate concern to environmental scientists.

In the following research work PPy-TSCP cation exchange nanocompsite was synthesized and applied in a simple electro analytical technique for detection/sensing of acetaldehyde vapors at ambient temperature.

2. Experimental

2.1. Chemical, reagents and instruments:

The following reagents were used as follows:

The pyrrole monomer (98%) from Spectrochem (India Ltd.), anhydrous iron(III)-chloride ($FeCl_3$), methanol HPLC grade Orthophosphoric acid (H_3PO_4), titanium dioxide (TiO_2), sulphosalicylic acid and ammonium sulphate were used as received from Qualigens (India Ltd.). All other reagents and chemicals were of analytical grade.

Ultrasonic vibrations (SC-I, Chengdu Jinzhou Ultrasonic Technology Co.), Fourier Transform Infra-red spectroscopy (FTIR) (Perkin Elmer 1725 instrument), Transmission electron microscopy (TEM) (JEOL TEM, JEM 2100F), field emission scanning electron microscopy (FE-SEM) and energy dispersive analyzer unit (EDAX) (LEO 435–VF), X–ray diffraction (XRD)(PHILIPS PW1710 diffractometer), Thermal analysis (TGA, DTA and DTG) (thermal analyzer-V2.2A DuPont 9900).

2.2 Synthesis of PPyTSCP Composite ion exchanger

2.2.1 Synthesis of Titanium(IV)sulphosalicylophosphate

Preparation of TSCP was carried out by taking different ratios of Titanium(IV)sulphate solution, aqueous solution of sulphosalicylic acid solution and aqueous solution of orthophosphoric acid prepared in demineralized water under varying conditions given in **Table 1**. Titanium(IV)sulphate solution was prepared by dissolving 2 g of titanium dioxide in 62.5 mL of hot concentrated sulfuric acid containing 25 g of ammonium sulphate with constant stirring **[18-19]**. While the reaction mixture was thoroughly stirred with a magnetic stirrer at room temperature (25 $^{\circ}$C), the solution containing precipitate was refluxed at 75–80 $^{\circ}$C for 24 h with constant stirring. The resulting precipitate was decanted and washed five times with demineralized water (DMW), filtered by suction and dried at 80±2 $^{\circ}$C for 24 h. Finally the material was dried in an oven at 80±2 $^{\circ}$C for 24 h in an oven. The material was finally grinded by pastel mortar to obtain fine powder of TSCP.

Sample code	Mixing volume ratio (v/v)		Appearance of the sample	Na^+ IEC ($meqg^{-1}$)
	Titanium Sulphosalicylic acid	Ortho-phosphoric acid (2 mol L^{-1})		
TSCP-1	1 (0.1 mol L^{-1})	1	White	1.20
TSCP-2	**1 (0.2 mol L^{-1})**	**1**	**White**	**1.40**
TSCP-3	1 (0.2 mol L^{-1})	2	White	1.30

Table 1: Conditions of preparation and the ion-exchange capacity TSCP cation exchanger.

2.2.2 Synthesis of Polypyrrole-titanium(IV)sulphosalicylophosphate Composite ion exchanger

PPy-TSCP nanocomposite was prepared by *in situ* chemical oxidative polymerization **[20, 21-24]** of pyrrole in presence of TSCP particles. A schematic representation of the formation of PPy-TSP nanocomposite is shown in **Scheme 1**. A certain amount of TSCP **[Table 2]** (dried at 50 ^oC for 2 h before use) was dispersed in approximately 100 mL of DMW under ultrasonic vibrations (SC-I, Chengdu Jinzhou Ultrasonic Technology Co.) at room temperature for 1 h. This TSCP dispersed solution was then diverted into a 500 mL single-necked round-bottom flask equipped with a magnetic, Teflon coated stirrer, and a certain amount of pyrrole monomer was added drop by drop using pipette. The mixture was stirred for 30 min for the adsorption of pyrrole on the surface of TSCP particles. The ferric chloride solution (2 g Ferric chloride in 100 mL of DMW) was added to the dispersion. This reaction mixture was further stirred for another 24 h under the same condition. The resultant PPy-TSCP nanocomposite powder was filtered with a Buchner funnel, and then washed with DMW to remove unreacted oxidant. It was further

washed thoroughly with methanol to remove any unreacted monomer and dried completely at 50 ^{o}C for further analysis. Pure PPy was synthesized by a similar method as the preparation of PPy-TSCP composites without the TSCP particles. The condition of preparation of the composite material and their ion-exchange capacities are given in **Table 2**.

Sample code	Titanium(IV) Sulphosalicylo Phosphate(g) (Sonicated in 100 mL DDW)	Iron(III)-chloride (g) (in 100 mL DDW)	Pyrrole monomer (mL)	Na^+ ion exchange capacity in ($meqg^{-1}$)	DC Electrical Conductivity (S/cm)
PTSCP-1	2.0	2.0	1.0	1.30	7.76×10^{-3}
PTSCP-2	2.0	2.0	3.0	1.00	7.89×10^{-3}
PTSCP-3	2.0	2.0	5.0	1.10	2.08×10^{-2}
PTSCP-4	**2.0**	**2.0**	**7.0**	**2.10**	**1.53×10^{-1}**
PTSCP-5	4.0	2.0	5.0	1.50	6.55×10^{-3}

Table 2: Conditions of preparation and the ion-exchange capacity of PPy-TSCP cation exchange nanocomposite.

2.3. Ion–exchange capacity (IEC)

IEC of each sample was determined by column method, IEC generally expressed as a measure of the H^+ ions liberated by neutral salt to flow through the composite cation exchanger. To

determine IEC one gram of dry ion-exchanger sample (in H^+–form) was loaded into a glass column with a glass wool supported at the bottom having an internal diameter ~1 cm and the bed length was approximately 1.5 cm long. Aqueous solution of sodium nitrate ($NaNO_3$) of 1 mol L^{-1} concentration was used as eluents to elute the H^+ ions completely from the cation exchange column, keeping a very slow flow rate (~ 0.5 mL min^{-1}). The effluent was titrated against a standard 0.1 mole L^{-1} NaOH solution using phenolphthalein as indicator. **Table 2** shows the ion-exchange capacity values of the samples.

2.4. Characterization

The Fourier transform infra-red spectroscopy (FTIR) spectra were recorded using Perkin Elmer 1725 instrument. To study the surface morphology, field emission scanning electron microscopy (FE-SEM) was done by LEO 435–VF. Transmission electron microscopy *(*TEM) was observed by JEOL TEM (JEM 2100F) instrument. X–ray diffraction (XRD) data was recorded by PHILIPS PW1710 diffractometer with Cu Kα radiation at 1.540Å in the range of $5^o \leq 2\theta \leq 70^o$at 40 kV. The thermal stability was investigated by thermal analysis (TGA, DTA and DTG) using thermal analyzer-V2.2A DuPont 9900. The samples were heated in alumina crucible from 30 ˚C to 1000 ˚C at the rate of 10˚C/min in the nitrogen atmosphere at the flow rate of 200 mL/min. The elemental analysis of PPy, TSCP and PPy-TSCP cation exchange nanocomposite was performed by using energy dispersive analyzer unit (EDAX) attached with FE-SEM.

2.5 Electrical conductivity and acetaldehyde sensing measurements

For electrical conductivity measurements and sensing experiments, 0.2 g material from each sample was pelletized at room temperature with the help of a hydraulic pressure instrument at 25

kN pressure for 5 minutes. DC electrical conductivity of nanocomposite was measured by using a four-in-line probe. The conductivity (σ) was calculated using the following equations **[22-24]**.

$$\rho = \rho_o / G_7 (W/S) \quad (1)$$

$$G_7 (W/S) = (2S/W) \ln 2 \quad (2)$$

$$\rho_o = (V/I)\, 2\pi S \quad (3)$$

$$\sigma = 1/\rho \quad (4)$$

Where G_7 (W/S) is a correction divisor which is a function of thickness of the sample as well as probe-spacing where I, V, W and S are current (A), voltage (V), thickness of the film (cm) and probe spacing (cm) respectively. In isothermal ageing experiments, the nanocomposite pellets were heated at 50, 70, 90, 110 and 130 ^{o}C in a PID controlled temperature oven. The electrical conductivity measurements were performed at an interval of 10 min. In cyclic ageing experiments, the DC electrical conductivity was measured in the temperature range of 40–150 ˚C repeatedly for five times at an interval of 1 h. Acetaldehyde vapours sensing measurements were done by monitoring the resistivity of the nanocomposite using the Laboratory made set-up for acetaldehyde sensing based on four-in-line probe electrical conductivity measuring instrument **[21-24].**

2.6 Acetaldehyde sensing kinetics.

For sensing kinetics 0.2 g selected pelletized material was taken at 15 and 20 °C temperatures and resistivity response was recorded by using four in line probe in atmosphere of acetaldehyde vapours with respect of time.

3. Results and discussion

3.1. Synthesis and conducting properties of Polypyrrole-titanium(IV)sulphosalicylophosphate Composite ion exchanger

Various samples of PPy-TSCP cation exchange nanocomposite were prepared by *in-situ* chemical oxidative polymerization of pyrrole in the presence of TSCP nanoparticles through electrostatic binding of negatively charged TSCP nanoparticles with partial positive charge of Hydrogen of NH group of the polymer as shown in **Scheme 1** under different conditions (**Table 2**).

The ion-exchanger (sample **PTSP-4**) possessed better Na^+ ion exchange capacity (2.10 $meqg^{-1}$) as compared to the inorganic TSCP (sample TSP-2, **Table 1**) (1.40 $meqg^{-1}$). The IEC of PPy-TSCP composite was increased due to addition of conductive polymer into the inorganic material (TSP) which increases the surface area of the material, thus exchangeable ionic sites were increased. Due to the better ion exchange capacity and electrical conductivity, sample **PTSCP-4 (Table 2)** was selected for further studies.

Variation in conductivity with different amount of loading of pyrrole monomer is shown in **Table 2**. High improvement in electrical conductivity and ion exchange capacity was found at 7mL loading of pyrrole monomer. The electrical conductivity of PPy-TSCP was found higher than PPy where as TSCP was observed as non conducting material. Since PPy-TSCP composite is an excellent ion exchanger (IEC 2.1 $meqg^{-1}$) that means it has abundant ionomeric sites present in the matrices of the material which may reasonably responsible for increase in conducting behavior of the material when it is in the protonated form. This increase in conductivity can be

well under stood from the percolative path (matrices of the material) in which the concentration of charge carriers of conducting ionomers increased.

3.2 Temperature dependence of DC electrical conductivity of the PPy and PPy-TSCP

The electrical conductivity of PPy and PPy-TSCP cation exchange nanocomposite was measured with increasing temperatures from 30 ˚C to 130 ˚C as shown in **Fig. 1.** The increase in conductivity with increase in temperature is the characteristic of ‘‘thermal activated behaviour’’ [**26**] this increase in conductivity may be due to the increase of efficiency of charge transfer between TSCP and polymer chains **[27-28].** It is also found that the thermal curing affects the chain alignment of the polymer, which leads to the increase of conjugation length, and that brings about the increase of conductivity. Also, there had to be molecular rearrangement on heating, which made the molecular conformation favourable for electron delocalization **[29].**

The conduction mechanism in the conducting polymers is explained in terms of polaron and bipolaron formation, since polymer at low level of oxidation gives polaron and higher level of oxidation gives bipolaron. Both polarons and bipolarons are mobile and move along the polymer chain by the rearrangement of double and single bonds in the conjugated system. Thus the mechanism of charge transport in polymer with non-degenerate ground states is mainly explained by conduction of polarons and bipolarons. The magnitude of the conductivity is dependent on the number of charge carriers available and their mobility. Increase in conductivity with the rise in temperature is due to increase in mobility of charge carriers. Molecular alignment of the chains within the entire system is another factor which also affects the electrical conductivity. The degree of the conductivity depends on both the number of charge carriers

and their mobility. It has been observed that mobility of charge carriers increases with the increase in temperature leading to the increase in conductivity similar to that reported for PANI/$WO_3$and PANI/CeO_2nanocomposites**[25-26]**.

.3. FTIR Analysis

The FTIR spectra of PPy, and PPy-TSCP nanocomposite are shown in **Fig. 2**. The FTIR spectra of PPy, in the finger print region of PPy shows absorption peak at 902 cm^{-1} which is characteristic of C–H out-of-plane deformation vibration, confirming the formation of PPy by the monomer. The band at 1300 cm^{-1} is attributed to the C–N in-plane, and the bands at 1167 and 1041 cm^{-1} are related to the C–H bending modes while the strong absorption band obtained at1539 cm^{-1} and 1449 cm^{-1} corresponds to the C–C stretching vibration in the pyrrole ring. Some other peaks in the fingerprint region (600-1500 cm^{-1}) can be attributed to the ring stretching and C–H in plane deformation mode. The PPy-TSCP nanocomposite shows a strong band at 3407 cm^{-1} may be attributed to the –OH stretching frequency and a broad band between 1250 and 800 cm^{-1} with a peak of intensity at 1042 cm^{-1} is due to presence of ionic phosphate group where as peak at 795 cm^{-1} is attributed to M–O bonding. The stretching vibration of C–N and C–C stretching vibration in pyrrole ring observed at 1325 cm^{-1} and 1559 cm^{-1} respectively indicates that the polymerization of PPy has been successfully achieved on the surface of the TSCP particles.

3.4 XRD pattern

The XRD patterns of PPy, TSCP and PPy-TSCP cation exchange nanocomposites are shown in **Fig. 3**. In the XRD pattern of pure PPy shows an obvious broad peak at $2\theta=30^{o}$, and some very low intensity peaks suggesting that PPy conducting polymer is amorphous in nature **[30].**The

broadening of peak of TSCP nanoparticle in PPy-TSCP nanocomposite suggests successful incorporation of TSCP nanoparticles in PPy-TSCP nanocomposite. The results are also in agreement with the FTIR and TEM studies.

3.5 Morphological studies

Fig. 4 shows the TEM image of TSCP and PPy-TSCP nanocomposite with granular morphology having an average particle size of ~20-40 nm and 30-50 nm respectively. The TSCP nanoparticles can be seen as dark spots encapsulated in PPy matrix. The FE-SEM images of TSP and PPy-TSCP nanocomposites are shown in **Fig. 5(a-d)** at different magnifications. **Fig. 5a** and **Fig. 5b** show the granular morphology, however the FE-SEM of PPy-TSCP nanocomposite **(Fig. 5c** and **Fig. 5d)** shows TSCP nanoparticles are well embedded in the polymer matrix with uniform dispersion. Thus, the results of XRD, FTIR, TEM and SEM studied have provided clear evidence that the polymerization of PPy has been successfully achieved on the TSCP nanoparticles. A schematic representation of the formation of PPy and PPy-TSCP nanocomposite is given in **Scheme 1**.

3.6 Thermo gravimetric analysis

The TGA curve of PPy, TSCP and PPy-TSCP nanocomposite is shown in **Fig. 6**. In case of PPy, the weight loss was observed in two stages at 200^{o}C (10.27%) and at 300^{o}C (14.05 %), the first one due to physisorbed water molecule and volatile impurities and in second one due to degradation of the polymer unsaturated groups. About 31.11 % weight was lost gradually up to 1000˚C due to degradation of polymer. In the case of TSCP, the first weight loss was observed at 100˚C (5.67%) due to removal of external water molecules and second weight loss up to 600˚C (17.54%) due to degradation of inorganic part of the material. After 600˚C the TSCP was found

stable up to 1000˚C (1.6% weight loss). In PPy-TSCP nanocomposite the first weight loss at 100˚C (5.67% weight loss) due to removal of external water molecules and second weight loss up to 900˚C (8.03% weight) because of degradation of PPy. The total loss of mass up to 1000˚C has been estimated to be about 65.43%, 23.37% and 38.64% for PPy, TSCP and PPy-TSCP respectively. On heating up to 1000˚C the amount of TSCP present in the PPy-TSCP matrix is calculated as 47.02% from the above data. The minimum loss Of TSCP from PPy-TSCP composite confirms that the presence of TSCP in PPy-TSCP nanocomposite is responsible for the higher thermal stability of the composite material in comparison to pristine PPy.

Fig. 7 shows the DTA curve of pure PPy, TSCP and PPy-TSCP nanocomposite. DTA curve of PPy, TSCP and PPy-TSCP indicate their endothermic peaks at near about 100 ˚C correspond to removal of external water molecules. One exothermic peak at ~300 ˚C in PPy and one exothermic peak at ~800 ˚C of PPy-TSCP are due to the polymeric degradation of material. However the maximum degradation of the composite material was observed at 800 ˚C. Thus results are in corresponds to the results of the TGA indicating thermal stability of PPy-TSCP composite material.

Fig. 8 shows DTG analysis of pure PPy, TSCP and PPy-TSCP nanocomposite was studied as a function of rate of weight loss ($\mu gmin^{-1}$) versus temperature. In case of pure PPy decomposition at 74 ˚C and 290 ˚C was found with 111 $\mu gmin^{-1}$ and 96 $\mu gmin^{-1}$ weight loss respectively and in case of TSCP decomposition at 109 ˚C and 529 ˚C was found with 94 $\mu gmin^{-1}$ and 529 $\mu gmin^{-1}$ weight loss respectively. However, in the case of PPy-TSCP nanocomposite, the decomposition was observed at 103, 971 ˚C with 133, 125 $\mu gmin^{-1}$ weight loss respectively. Thus, it could be inferred from the DTG studies that the rate of thermal decomposition was higher in the case of pristine PPy, where as in the case of PPy-TSCP the rate of thermal decomposition is lower. The

better thermal resistance of pure PPy-TSCP nanocomposite was due to incorporation of TSCP in the PPy matrix.

3.7 Energy dispersive x-ray analysis

The EDAX patterns of PPy and PPy-TSCP cation exchange nanocomposites are shown in **Fig. 9**. EDAX studies have provided clear evidence that the polymerization of PPy has been successfully achieved on the of the TSCP nanoparticles. The percent compositions of elements are given in **Table 3.**

Element	Weight (%)		
	PPy	TSCP	PPy-TSCP
C	64.73	20.25	28.66
N	19.04	-	7.80
O	16.23	19.86	37.04
Ti	-	34.09	15.44
P	-	24.20	10.75
S	-	1.60	0.30

Table 3. Percent composition of elements present in PPy-TSCP nanocomposite by EDAX analysis.

3.8 Stability in terms of DC electrical conductivity retention

The stability in terms of DC electrical conductivity retention of the PPy and PPy-TSCP nanocomposite was studied by isothermal aging and cyclic aging techniques in ambient atmosphere.

3.8.1 DC electrical conductivity retention under isothermal aging conditions

The isothermal stability of the composite material in term of DC electrical conductivity retention was carried out at 50 ˚C, 70 ˚C , 90 ˚C, 110 ˚C and 130 ˚C in an air oven. The electrical conductivity measurements were done five times after an interval of 10 min at a particular temperature. The electrical conductivity measured with respect to time is depicted in **Fig.10**. It was observed that all the composite materials followed Arrhenius equation for the temperature dependence of the electrical conductivity from 50 to 90 ˚C and after that a deviation in electrical conductivity was observed, it may be due to the loss of polymer and degradation of materials. The isothermal stability in terms of DC electrical conductivity retention of PPy-TSCP cation exchange nanocomposite was found to be better than pristine PPy which suggests that the PPy-TSCP cation exchange nanocomposite may be used in electrical and electronic devices below 100 ˚C under ambient conditions.

3.8.2 DC electrical conductivity retention under cyclic aging conditions

The stability in terms of DC electrical conductivity retention of PPy and PPy-TSCP cation exchange nanocomposite was also studied by cyclic aging technique. From **Fig. 11** it may be observed that the DC electrical conductivity at the beginning of each cycle was found to be low than the previous cycle which further decreases with increase in number of cycle for PPy and PPy-TSCP cation exchange nanocomposite. This may be due to the loss of moisture and polymer degradation during cyclic aging. From cyclic electrical conductivity study on PPy **[Fig 11(a)]** and PPy-TSCP **[Fig 11(b)]** cation exchange nanocomposite suggests that the electrical conductivity of the nanocomposite is more stable than pristine PPy.

3.9 Acetaldehyde vapour sensing of PPy-TSCP nanocomposite.

The acetaldehyde vapours sensing performance of PPy-TSCP (PTSP-4) cation exchange nanocomposite was monitored by measuring resistivity changes on exposure to acetaldehyde vapours using laboratory made assembly designed by using 4-in-line probe electrical conductivity device. The electrical resistivity of the cation exchange nanocompsiteas a function of time showed remarkable changes on exposure to different concentrations (0.1M, 0.3M, 0.5M, and 0.7M) of aqueous acetaldehyde at room temperature are shown in **Fig. 12 (a)**. It can be seen that the nanocomposite showed a relatively fast response towards aqueous acetaldehyde of 0.7 M concentration (vapour concentration 2.95%) and the resistivity can be recovered on flushing in air. The response and recovery time of the sensor was around 5 sec for 0.7 M aqueous acetaldehyde. The reversibility of the nanocomposite was also investigated and the response of the nanocomposite towards 0.7 M aqueous acetaldehyde was found to be highly reversible during the test of cyclic measurement as shown in **Fig. 13**. The duration of acetaldehyde air cycle is short (5 s) so the resistance after each cycle doesn't recover. There is interaction of lone pair of oxygen of acetaldehyde with carbon of PPy, which decreases the intensity of positive charge and hence the mobility of charge carriers decreases resulting in the increase in resistivity. If time of air flush increases the resistivity may recover due to the loss of acetaldehyde vapours although a little bit of irreversibility can be observed.

If polpyrrole is not doped with TSCP then polymer do not sense in the same manner as Polypyrrole titanium(IV) sulphosalicylophosphate (PPy-TSCP). From **Fig. 12(b)** it is depicted that rate of change in resistivity response with time on exposure to Acetaldehyde vapours is not same as that of PPy-TSCP. Total change in resistivity of polypyrrole is 0.0116 S/cm and in PPy-TSCP is 0.04599 S/cm.

From experimental data it can be suggested that PPyTSCP show good sensing performance on exposure to Acetaldehyde as compare to Polypyrrole.

When mixture of same concentration of acetaldehyde and formaldehyde was sensed by PPyTSCP, the resistance profile changed shown in **Fig 12 (c)**. The change in resistance profile may be due to dipole-dipole force of attraction between partial positive hydrogen of formaldehyde and partial negative oxygen of acetaldehyde. Due to dipole-dipole force of attraction less vapours formation take place from aqueous media which effect the resistance profile

The degree of reversibility of the sensor was checked by repetitive cyclic measurements using 0.7M aqueous acetaldehyde solution. The relative standard deviation (RSD %) of 0.7M was calculated to be 1.62%. It can be concluded from the RSD (%) that the sensor works best for 0.7M concentration.

3.10 Second order kinetics evaluation for acetaldehyde sensing on PPy-TSCP nanocomposite and kinetic parameters.

Order of reaction of acetaldehyde vapour sensing on PPy-TSCP nanocomposite was evaluated for the physical interaction of acetaldehyde on PPy-TSCP nanocomposite. The mechanism of interaction may explain on the basis of the electrostatic interaction of lone pair of oxygen in acetaldehyde with carbon in PPy of PPy-TSCP nanocomposite. To ascertain the order of the reaction, the standard equation for first and second were applied as give below

$$\mathbf{Log\ C = log\ C_0 - (}k_1\mathbf{/2.303)}\ t \quad \mathbf{(5)}$$

$$\mathbf{1/C - 1/C_0} = k_1 t \quad \mathbf{(6)}$$

Where C is the conductivity (reverse of resistivity) response recorded during sensing, C_0 is the conductivity at the start of the sensing, k_1 is the rate constant, and t is the time.

A tentative explanation of process occurring on the surface of PPy-TSCP can be explained as the lone pair of oxygen of acetaldehyde interacts with the carbon of PPy, which decreases the intensity of positive charge and hence the mobility of charge carriers decreases resulting in the decrease in conductivity. The mechanistic representation of the electrical compensation of PPy in the PPy-TSCP nanocomposite in the present work is given in **Scheme 2**. Conductivity vs. time and reverse of conductivity vs. time graph for sensing of acetaldehyde vapours on PPy-TSCP in **Fig.14** and **15** shows straight line pattern in which **Fig 14** most resemble with first order reaction.

Rate constant K_1 (0.0018 S^{-1}) and K_2 (0.0030 S^{-1}) at 15 ˚C and 20 ˚C were determined from the slopes of the graph of inverse of conductivity verse time in **Fig 16.**

According to the transition state theory presented by Laidler **[31]** the rate constant for a process can be written as

$$K = K_B T/h \; e^{(\Delta S^*/R)} \; e^{(-\Delta H^*/RT)} \qquad (7)$$

Where K_B is Boltzmann's constant, h is Plank's constant, T is absolute temperature, ΔS* is the entropy of activation, ΔH* is the enthalpy of activation, and R is gas constant.

The Arrhenius activation energy, Ea is determined from Arrhenius equation at two different temperatures.

$$\ln K_1/K_2 = Ea/R\,(1/T_1 - 1/T_2) \qquad (8)$$

The enthalpy of activation, ΔH*, can be calculated from the relationship:

$$\Delta H^* = Ea - RT \qquad (9)$$

The entropy of activation ΔS* was calculated from equation (7) and the free energy of activation ΔG* was determined from:

$$\Delta G^* = \Delta H^* - T\Delta S^* \qquad (10)$$

Results are summarized in **Table 4** the negative value of ΔS* and positive value of ΔH* indicate the feasibility and endothermic behavior during sensing process.

Temperature (°C)	Rate constant *K*(l mol^{-1} s^{-1})	Ea* (kcal mol^{-1})	ΔH* (kcal mol^{-1})	ΔG* (kcal mol^{-1})	ΔS* (cal K^{-1} mol^{-1})
15	1.8 x 10 $^{-3}$	18.36	17.787	20.452	-9.251
20	3.0 x 10^{-3}		17.777	20.501	-9.297

Table 4. Kinetic parameters for the acetaldehyde sensing on PPy-TSCP cation exchange nanocomposite

3.11 Sensing mechanism

Interaction of acetaldehyde with PPy in the PPy-TSCP nanocomposite is almost a reversible process, although a little bit of irreversibility can also be observed. The value of resistivity increased by the interaction of acetaldehyde with PPy and under ambient conditions the resistivity can be restored. However, the resistivity never came back to its original value and it was always found higher than the previous value for higher concentration of acetaldehyde. Thus it can be concluded that there are two processes in operation, firstly reversible chemisorption of acetaldehyde with PPy occurs and secondly compensation or electrical neutralization of the polymer backbone takes place.

In the light of observation by Ansari and co-worker**[1]** in their nanocomposite of polyaniline with TiO_2 it can be inferred that the lone pair of oxygen of acetaldehyde interacts with the carbon of PPy, which decreases the intensity of positive charge and hence the mobility of charge carriers decreases resulting in the increase in resistivity. Since the exposure to acetaldehyde was carried out in closed system and chemical linking is much more complicated process, desorption of acetaldehyde also occurs readily under ambient conditions and thus the resistivity is restored.

On exposure to acetaldehyde for long duration, complete electrical neutralization of the polymer backbone occurred. The mechanistic representation of the electrical compensation of PPy in the PPy-TSCP nanocomposite in the present work is given in **Scheme 2**.

4. Conclusion

In the present work, the Polypyrrole-titanium(IV)sulphosalicylophosphate cation exchange nanocomposites exhibiting acetaldehyde vapour sensing properties have been successfully synthesized by using an in-situ chemical oxidative polymerization technique. The results of Fourier Transform Infra-red spectroscopy, Transmission electron microscopy, field emission scanning electron microscopy, energy dispersive analyzer unit and thermal analysis studies reveal that the polymerization of pyrrole has been successfully achieved on the surface of titanium(IV)sulphosalicylophosphate particles and indicates that there is a strong interaction between Polypyrrole and titanium(IV)sulphosalicylophosphate particles. The Polypyrrole-titanium(IV)sulphosalicylophosphate cation exchange nanocomposites show improved thermal stability as well as ion exchange capacity in comparison with the pure Polypyrrole. The reproducible acetaldehyde vapours sensing results in the range of 0.1 to 0.7M aqueous

Acetaldehyde indicate that Polypyrrole-titanium(IV)sulphosalicylophosphate nanocomposite can be used in making a sensing device.

Sensing kinetics of acetaldehyde vapour on Polypyrrole-titanium(IV)sulphosalicylophosphate was also studied and it was found that acetaldehyde vapour sensing on Polypyrrole-titanium(IV)sulphosalicylophosphate follow second order of kinetics.

Acknowledgements

Authors are thankful to the University Grants Commission (India) for major Research project [42-336/2013], MANF and Department of Applied Chemistry for providing financial support and research facilities.

References:

[1] M.O. Ansari, F. Mohammad, Sens. Actuators B: Chem., 2011, 157, 122– 129.

[2] R. Gangopadhyay, A. De, Chem. Mater. 12 (2000) 608-622.

[3] T. Zhang, Y. He, R. Wang, W. Geng, Sens. Actuators B: Chem., 2008, 131, 687-691.

[4] K. Majid, R. Tabassum, A.F. Shah, S. Ahmad, M.L. Singla, J. Mater. Sci. Mater. Electron., 2009, 20,958-966

[5] J. Janata, M. Josowicz, Nat. Mater., 2003, 2, 19-24.

[6] L.W. Shacklette, N.F. Colaneri, V.G. Kulkarni, B. Wessling, J. Vinyl Tech., 1992, 14, 118-122.

[7] J. Huang, X. Wang, A.J. de Mello, J.C. de Mello, D.D.C. Bradley, J. Mater. Chem., 2007, 17, 3551-3554.

[8] K. Gurunathan, A.V. Murugan, R. Marimuthu, U.P. Mulik, D.P. Amalnerkar, Mater. Chem. Phys., 1999, 61, 173-191

[9] Y.Hou, Y. Cheng, T. Hobson, and J. Liu, Nano Lett., 2010, 10, 2727–2733

[10] Y.J. Yuan, S.B. Adeloju, G.G. Wallace, Eur. Polym. J., 1999, 35, 1761-1772.

[11] H.Y. Mi, X.G. Zhang, X.G. Ye, S.D. Yang, J. Power Sources, 2008, 176, 403-409.

[12] S. Biswas, L.T. Drzal, Chem. Mater., 2010, 22, 5667-5671.

[13] A. A. Khan, L. Paquiza, J.Ind. Eng Chem., 2014, 20, 4261-4266.

[14] J. Han, L.Y. Li, P. Fang, R. Guo, J. Phys. Chem. C, 2012, 116, 15900-15907.

[15] C.P. de Melo, B.B. Neto, E.G. de Lima, L.F.B. de Lira, J.E.G. de Souza, Sens. Actuators B: Chem. 2005, 109, 117-380

[16] S. Deki, K. Akamatsu, T. Yano, M. Mizuhata and A. Kajinami, J. Mater. Chem., 1998, 8(8), 1865–1868

[17] Huang, Jan-chan, Adv. Polym. Technol.,2002, 21, 299-313.

[18]. A.A khan, U. baig, J. Ind. Eng. Chem., 2012, 18 1937-1944.

[19] M. O. Ansari, F. Mohammad, Sens. Actuators B: Chem., 2011, 157, 122-129.

[20] A.A. Khan, U. Baig, Composites: Part B, 2014, 56, 862-868.

[21] A. A.Khan, U. Baig, Sens. Actuators, 2013, 177, 1089-1097

[22] A.A. Khan, M. Khalid, U. Baig, React. Funct. Polym., 2010, 70, 849–855.

[23] A. A.Khan, U. Baig, J. Hazard. Mater., 2011, 186, 2037–2042.

[24] M. Shakir, N. e. Iram, M. S. Khan, S. I. Al-Resayes, A. A. Khan, U. Baig, Ind. Eng. Chem. Res., 2014, 53, 8035-8044.

[25] N. Parvatikar, S. Jain, S.V. Bhoraskar, M.V.N.A. Prasad, J. Appl. Polym. Sci., 2006, 102, 5533–5537.

[26] N. Parvatikar, S. Jain, S. Khasim, M. Revansiddappa, S.V. Bhoraskar, M.V.N.A. Prasad, Sens. actuators B: Chem., 2006, 114, 599-603.

[27] M. Leclerc, G. D'Aparno, G. Zotti, Synth Met., 1993, 55, 1527.

[28] F. Zuo, M. Angelopoulos, A. G. MacDiarmid, A. Epstein, A. J. Phys Rev B., 1987, 36, 3475.

[29] A. Kobayashi, H. Ishikawa, K. Amano, M. Satoh, E. Hasegawa, J Appl Phys., 1993, 74, 296.

[30] L. Hong, Y.li, M.Yang, Sens. Actuators B: Chem., 2010, 145, 25-31.

[31] K.J. Laidler, Chemical Kinetics, McGraw-Hill, New York, 1965, 556.

Table of content:

S.No.	Figures contents
1	Temperature dependence electrical conductivity of PPy and PPy-TSCP nanocomposite
2	FTIR spectra of PPy and PPy-TSCP cation exchange nanocomposite.
3	XRD patterens of PPy, TSCP and PPy-TSCP cation exchange nanocomposite.
4	TEM image of (a) TSCP, selected area diffraction pattern (SAED) of (a) TSCP, TEM image of (b) PPy-TSCP nanocomposite and selected area diffraction pattern (SAED) of (b) PPy-TSCP nanocomposite.
5	FE-SEM images of (a-b) TSCP and (c-d) PPy-TSCP nanocomposite at different magnifications
6	TGA curves of PPy, TSCP and PPy-TSCP cation exchange nanocomposite.
7	DTA curves of PPy, TSCP and PPy-TSCP cation exchange nanocomposite.
8	DTG curves of PPy, TSCP and PPy-TSCP cation exchange nanocomposite.
9	EDX Spectra of PPy and PPy-TSCP cation exchange nanocomposite
10	Isothermal stability of (a) PPy and (b) PPy-TSCP nanocomposite in terms of D.C. electrical conductivity retention at 50^{o}, 70^{o}, 90^{o}, 110^{o}, and 130 ^{o}C
11	DC electrical conductivity of (a) PPy and (b) PPy-TSCP nanocomposite in terms of cyclic ageing conditions
12(a)	Effect on the resistivity of PPy-TSCP nanocomposite on exposure to different concentrations of acetaldehyde with respect to time.
12(b)	Effect on the resistivity of Polypyrrole on exposure to acetaldehyde vapours at 0.7M concentration of acetaldehyde with respect to time
12(c)	Effect on the resistivity of PPyTSCP on exposure to acetaldehyde and formaldehyde vapours of 0.7M concentration and pure acetaldehyde vapours of 0.07M concentration with respect to time
13	Reversible resistivity response curve of PPy-TSCP nanocomposite towards 0.7M acetaldehyde solution.
14	Conductivity versus time graph for evaluating first order reaction
15	Conductivity versus time graph for evaluating second order of reaction
16	Rate constant K_1 and K_2 at temperature 15 ^{o}C and 20 ^{o}C from the slope of the graph K = - slope, $K_1 = 0.0018\ S^{-1}$, $K_2 = 0.0030\ S^{-1}$
Scheme 1	Schematic diagram of the formation mechanism of (a) PPy and (b) PPy-TSCP nanocomposite
Scheme 2	The schematic diagram showing the chemisorption (reversible) interaction of PPy acetadehyde in the PPy-TSCP nanocomposite.

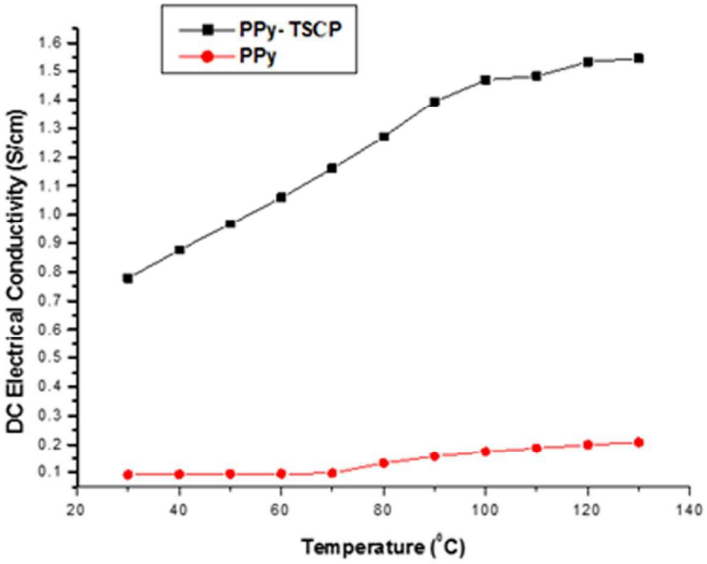

Fig. 1

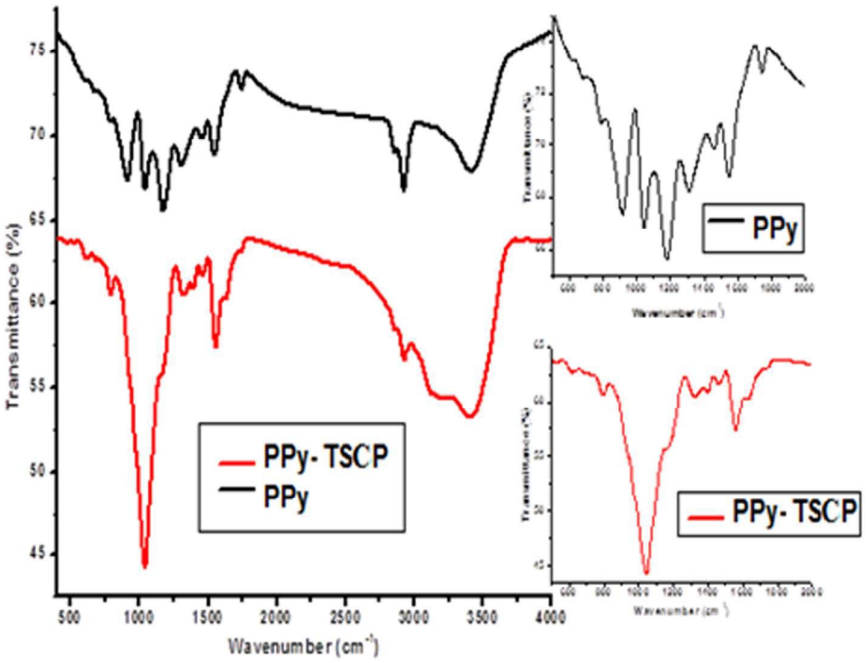

Fig. 2

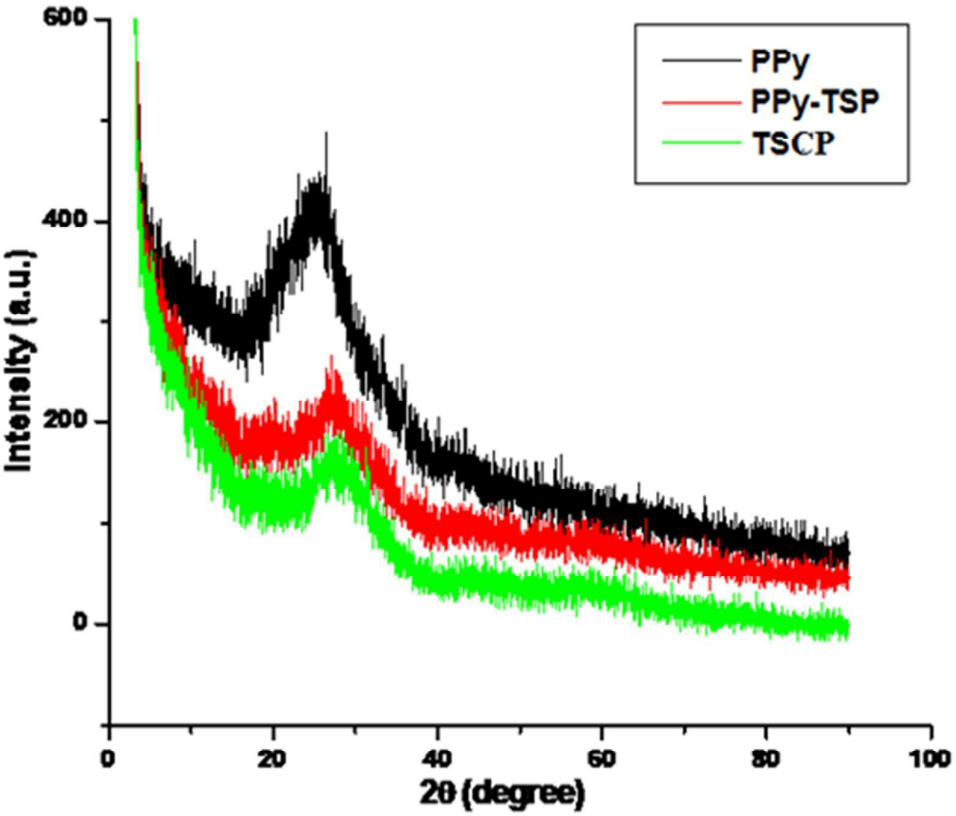

Fig. 3

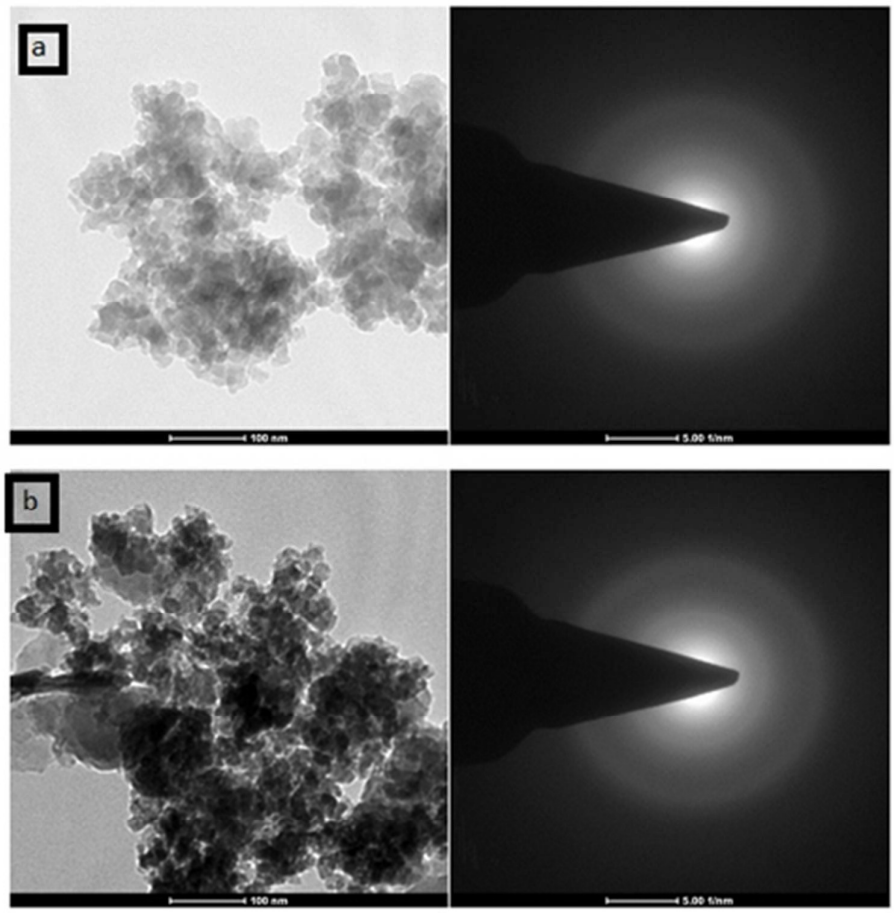

Fig. 4

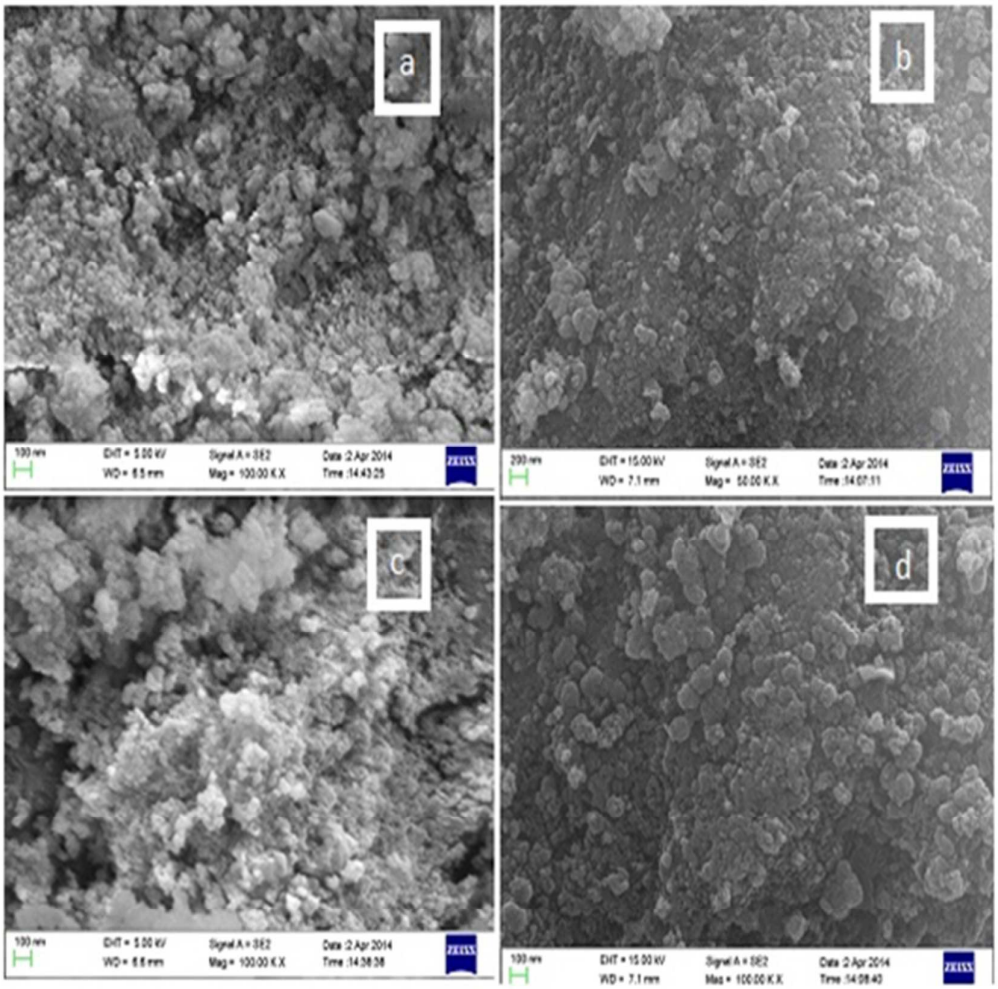

Fig. 5

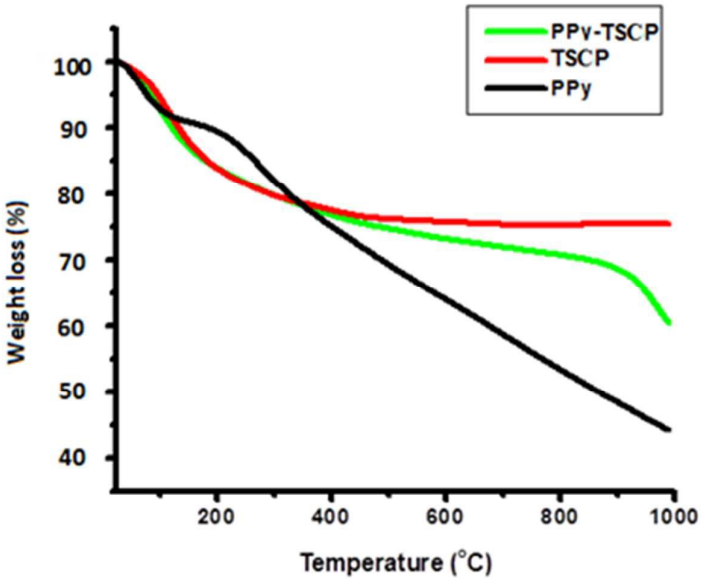

Fig. 6

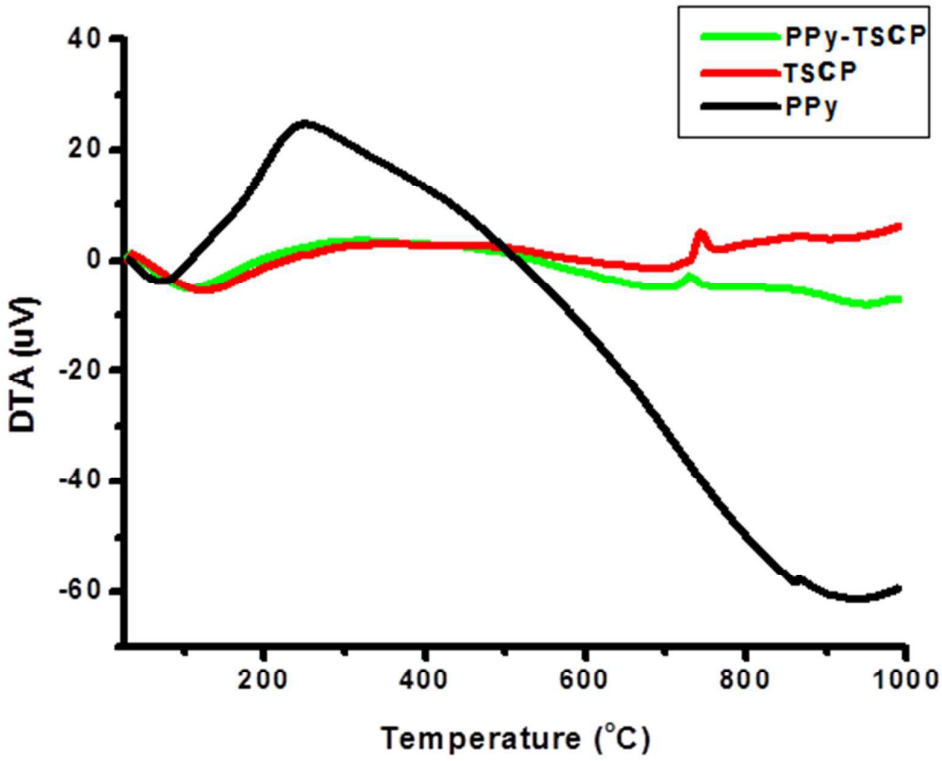

Fig. 7

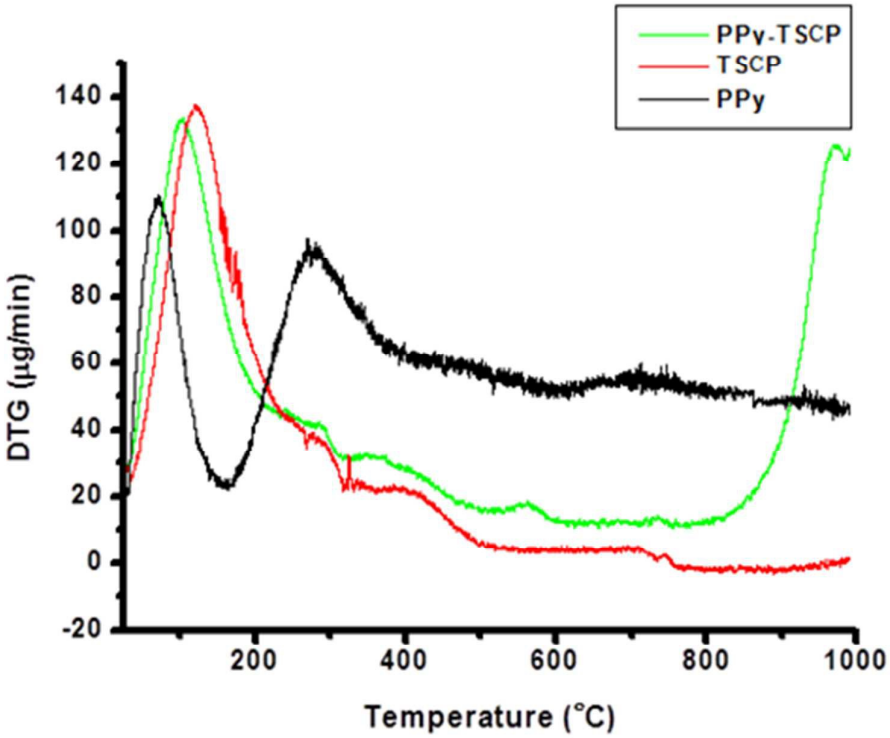

Fig. 8

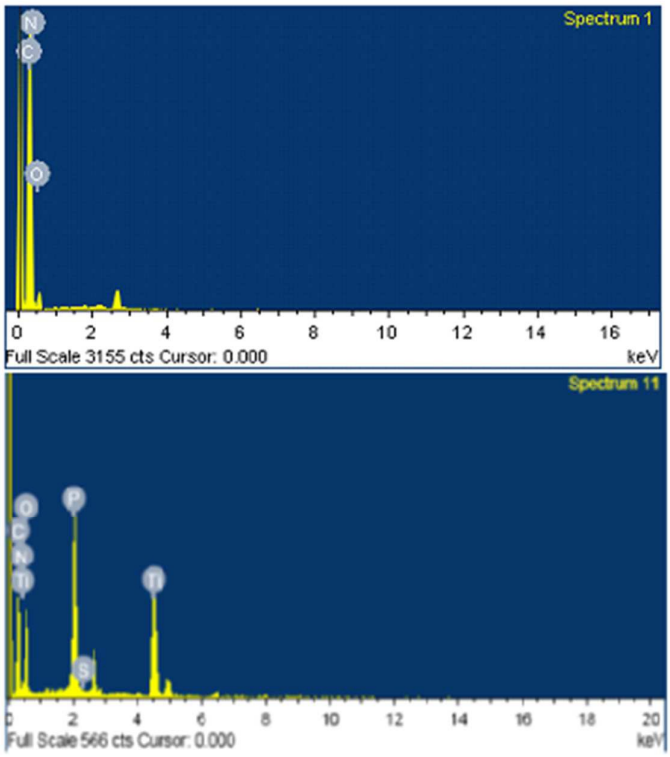

Fig. 9

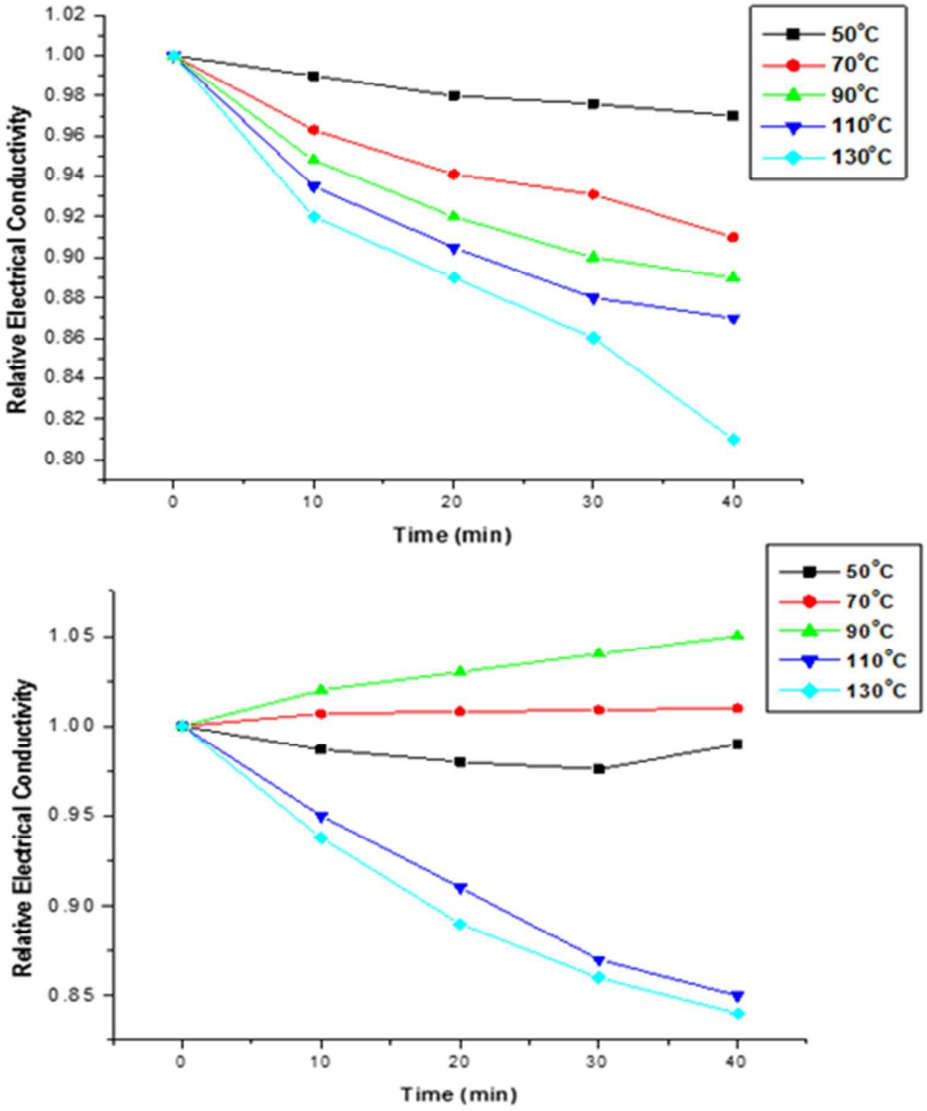

Fig. 10

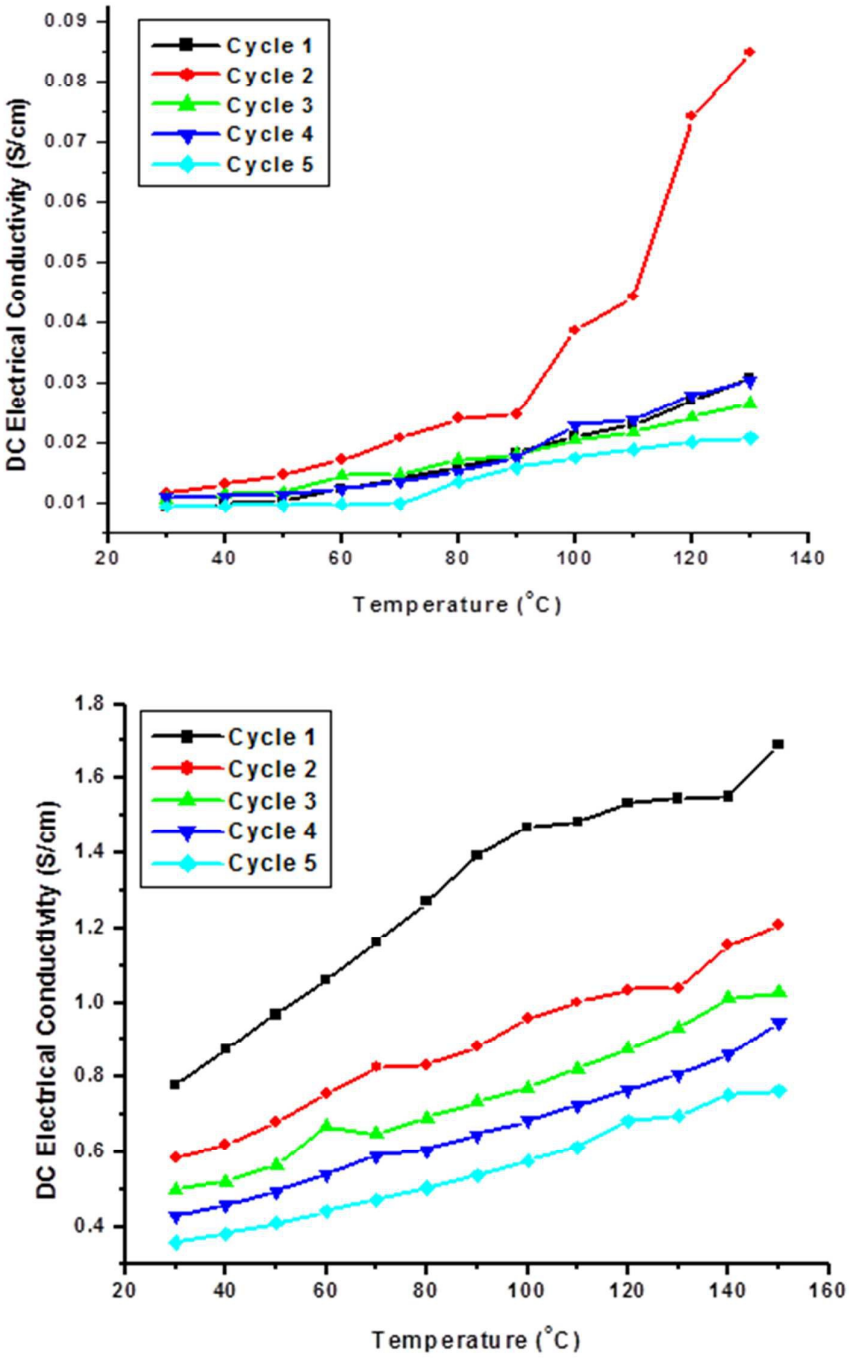

Fig. 11

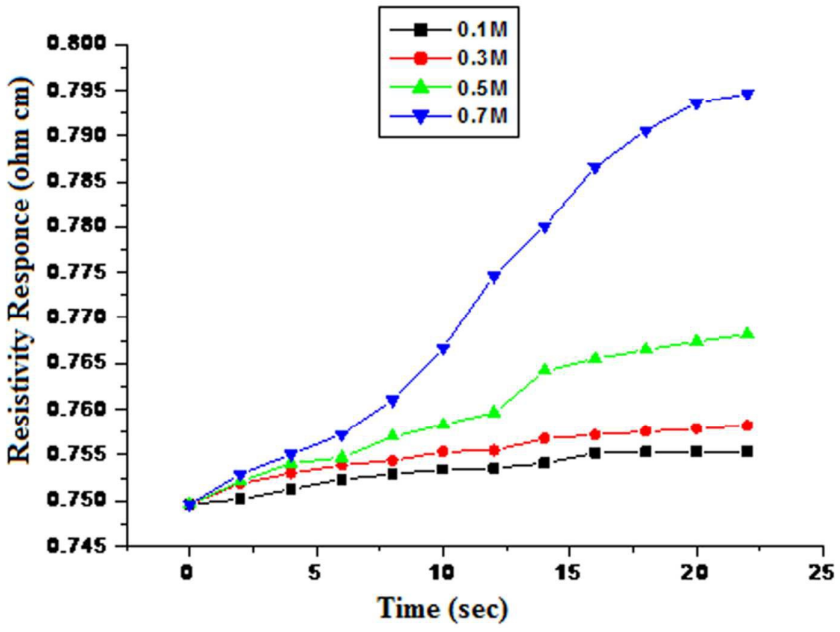

Fig. 12(a)

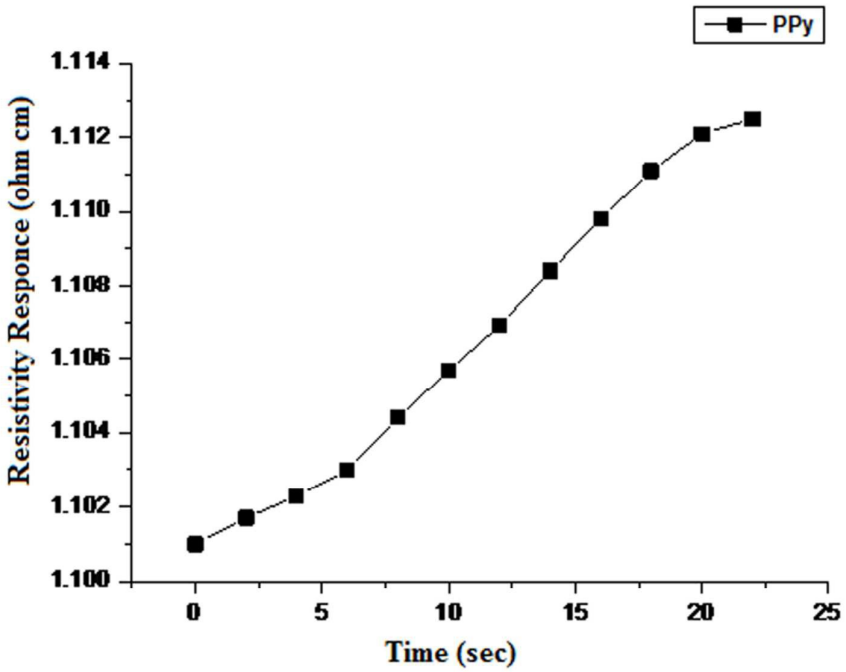

Fig. 12(b)

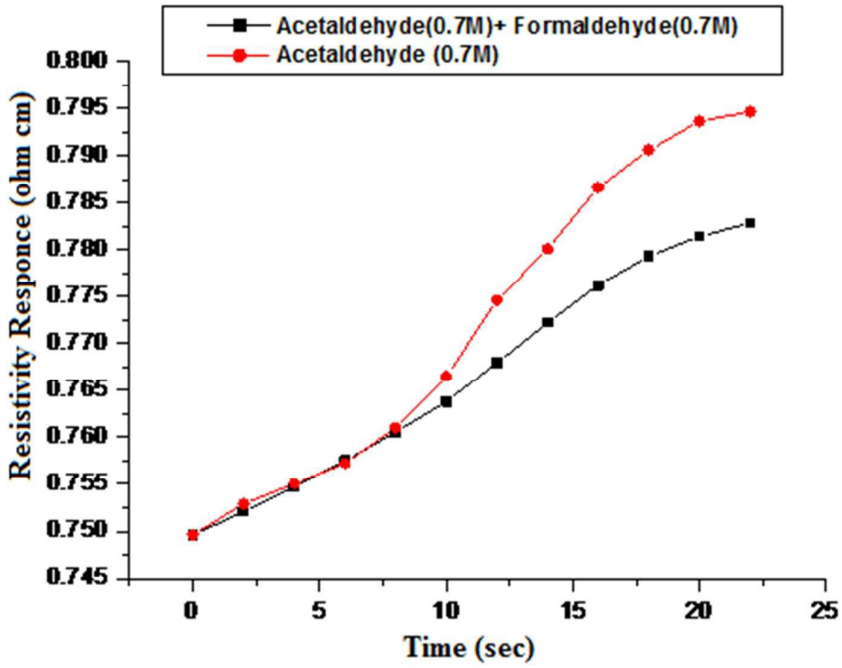

Fig.12 (c)

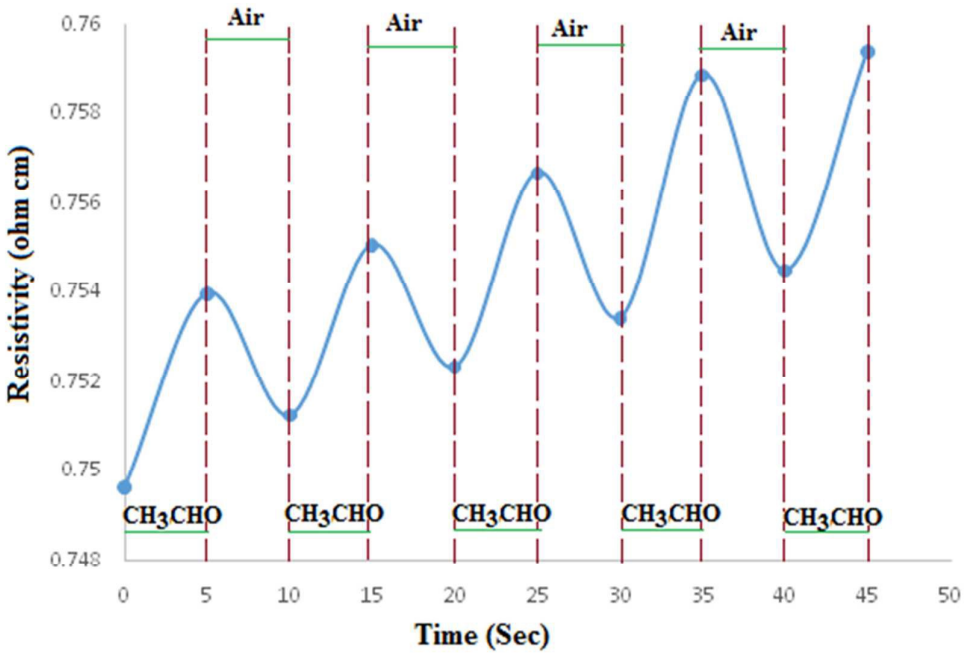

Fig. 13

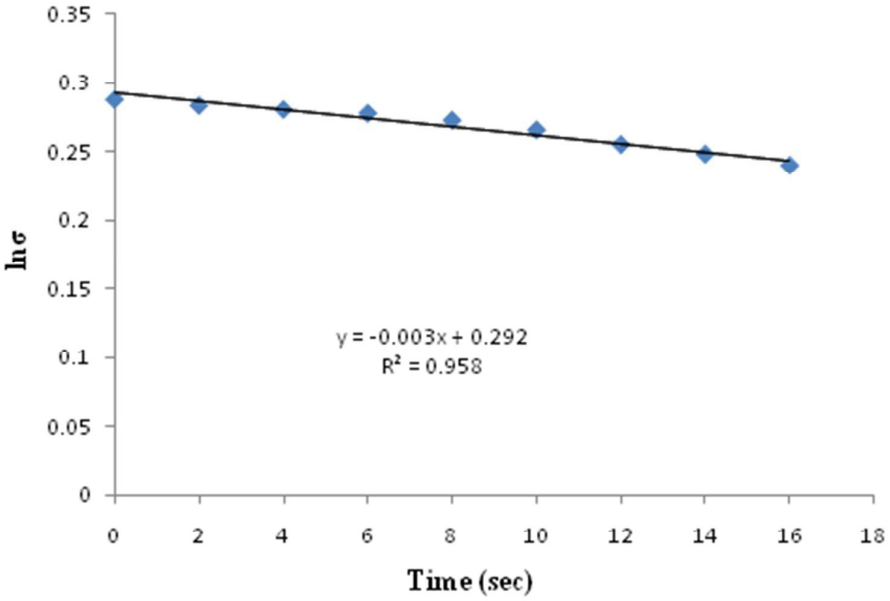

Fig. 14

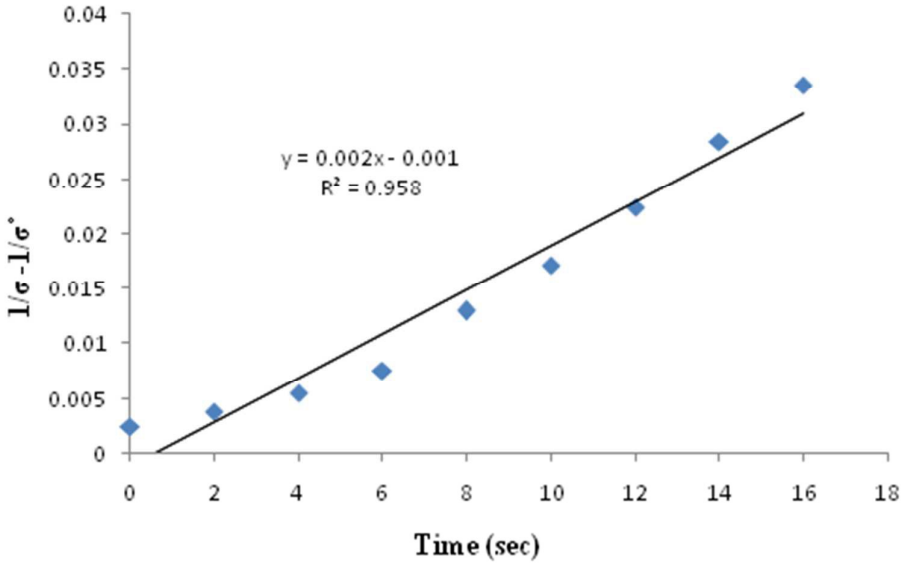

Fig. 15

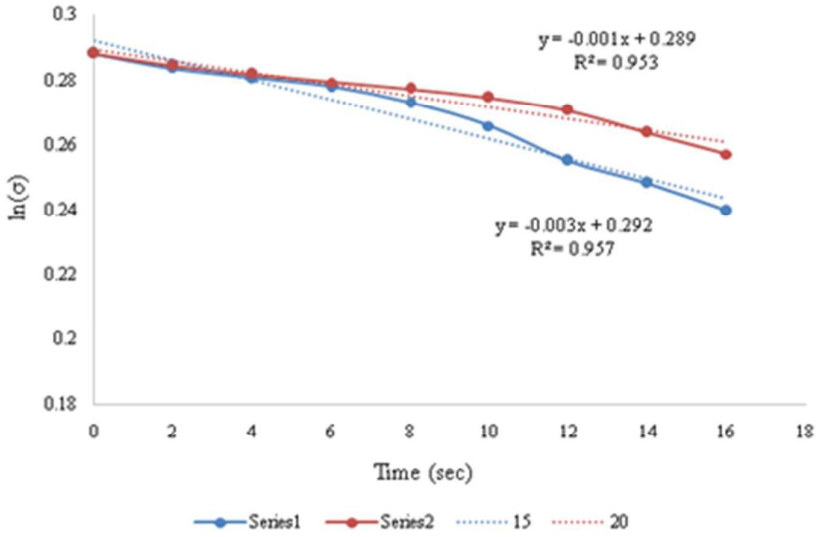

Fig. 16

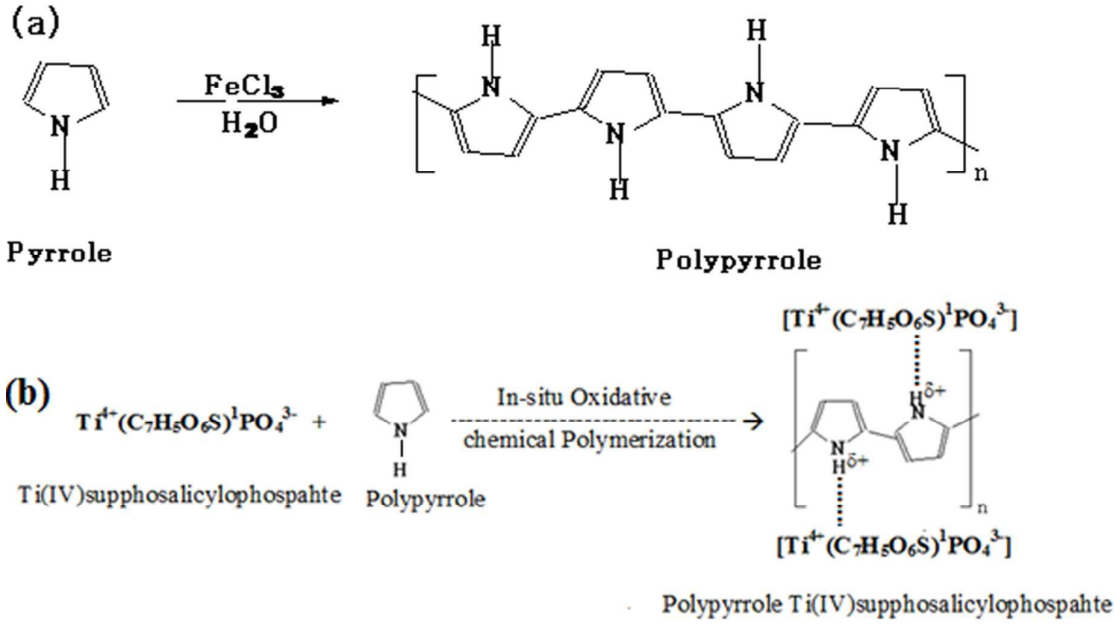

Scheme .1

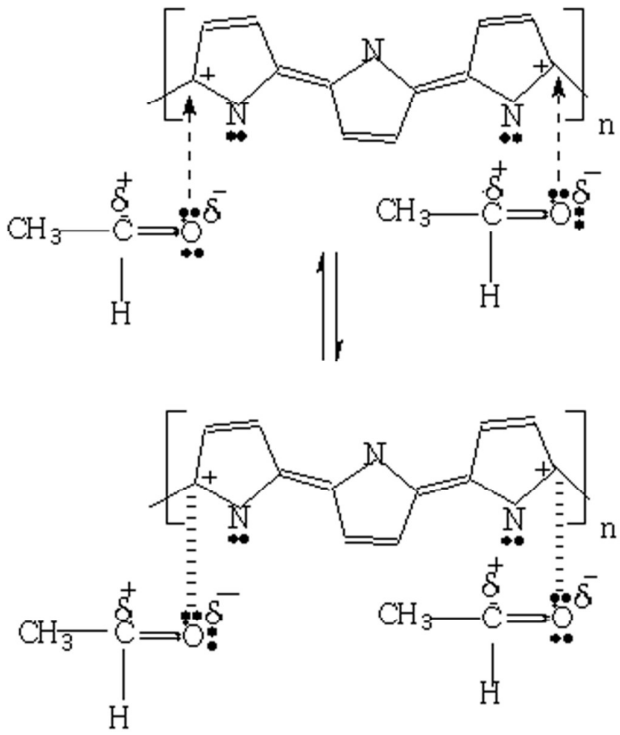

Scheme 2

Graphical Abstract:

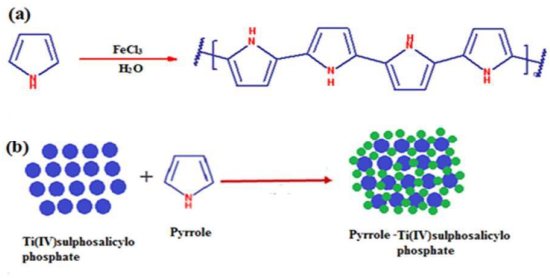

Highlights:

Polypyrrole-Titanium (IV)sulphosalicylophosphate composite is a better sensing as well as conducting material then Polypyrrole in semiconducting range.